Journal of Spacecraft and Rockets
Vol. 56, No. 3, May–June 2019

Engineering Notes

Modeling Temperature Variations of the Deep Space Climate Observatory

Robert E. Harpold,* Edward Malinowski,*
and Alexander Bounitch†
ASRC Federal Technical Services, Beltsville, Maryland 20705
Craig E. Roberts‡
KBRwyle, Lanham, Maryland 20706
and
Richard Malmstrom§
Northrop Grumman Innovation Systems, Dulles, Virginia 20166

DOI: 10.2514/1.A34335

I. Introduction

THE Deep Space Climate Observatory (DSCOVR) was launched on 11 February 2015 and entered a Lissajous orbit around the Earth–moon/sun L_1 Lagrange point on 8 June 2015. A Lissajous trajectory is not a closed orbit, and so it does not repeat with each revolution [1]. DSCOVR's orbit amplitudes are $A_x = A_y =$ 281,476 km and $A_z = 160{,}538$ km [2], and it has an orbital period slightly less than half a year. The spacecraft maintains Earth pointing, which requires changing pitch, roll, and yaw angles with respect to the sun throughout the orbit [3]. It carries the instruments National Institute of Standards and Technology Advanced Radiometer for measuring the received radiation on Earth's sunlit side, Earth Polychromatic Imaging Camera for taking images of Earth, and Plasma-Magnetometer for measuring the solar wind.

DSCOVR controls its temperature primarily through materials with low solar absorptivity, as well as using radiators and multilayer insulation (MLI) blankets. Some subsystems use heaters to maintain temperatures within operational ranges [4]. Several factors can damage the MLI blankets or change the spacecraft surface properties, including radiation, micrometeoroids, and solar events [5]. Therefore, the spacecraft's temperatures are expected to change throughout the mission lifetime.

The computational hub (comphub), which is used for command and data handling [6], and the fuel tank both have annual patterns in their temperatures (Fig. 1). Because both components have similar patterns, it is expected that orbit and attitude are the main factors, rather than internal effects.

Fuel-tank temperature and pressure are used to model thruster performance when planning station-keeping maneuvers to maintain the Lissajous orbit. Changes in comphub temperature affect the clock drift rate. The clock drift rate is expected to change, and will remain within acceptable bounds if the comphub temperature remains between 10 and 30°C [7]. The ability to predict fuel tank and comphub temperatures will allow better prediction of thruster performance during maneuvers, as temperature is a factor in thruster performance, and better prediction of when clock updates will be required.

In addition, the fuel tank has operating limits of 10–40°C, and the comphub has operating limits between −20 and 50°C [4]. Having a reliable temperature prediction for those subsystems will allow the operators to react beforehand if temperatures are predicted to go outside the operating limits.

II. Analysis

Frequency analyses of the fuel-tank temperatures (Fig. 2) and the comphub temperatures (Fig. 3) show peaks at two and eight cycles per 370 days, with a small peak at 18 cycles per 370 days. The cycles at those peaks correspond to periods of 335, 83.75, and 37.22 days, and were hypothesized to correspond to orbital parameters.

Because the spacecraft's distance with respect to the sun varies throughout the year, the ambient temperature will change. Figure 4 shows the fuel-tank temperature and the distance from the sun in the ecliptic plane. (There are negligible differences between using the total distances or the in-ecliptic distances.) It can be seen that the minimum annual temperatures correspond to DSCOVR's maximum annual distances from the sun and vice versa, which roughly correspond to the 335-day cycle. There are cycles within that cycle, and their extrema imply that temperature is additionally affected by factors other than distance from the sun.

Figure 5 shows the fuel-tank temperature and DSCOVR's out-of-ecliptic distance. There are correlations between distance and temperature extrema, but the correlations are not as strong as those for DSCOVR's distance from the sun. It can be seen that the out-of-

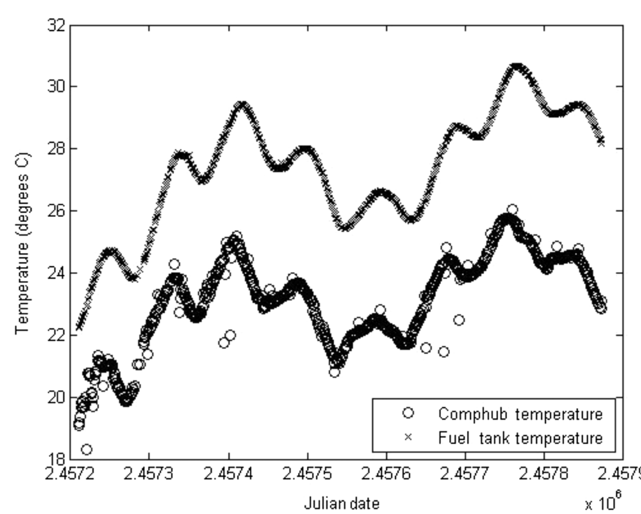

Fig. 1 DSCOVR comphub and fuel-tank temperatures.

Received 19 June 2018; revision received 22 November 2018; accepted for publication 17 January 2019; published online Open Access 13 February 2019.

*EMOSS DSCOVR Flight Dynamics Engineer, National Oceanic and Atmospheric Administration (NOAA), Engineering and Mission Operations Support Services V Contract, NOAA Satellite Operations Facility, 4231 Suitland Road, Suitland, MD.

†EMOSS DSCOVR Flight Software Engineer, National Oceanic and Atmospheric Administration (NOAA), Engineering and Mission Operations Support Services V Contract, NOAA Satellite Operations Facility, 4231 Suitland Road, Suitland, MD.

‡Principal Systems Engineer, 7515 Mission Drive.

§Senior Systems Engineer, 45101 Warp Drive. Member AIAA.

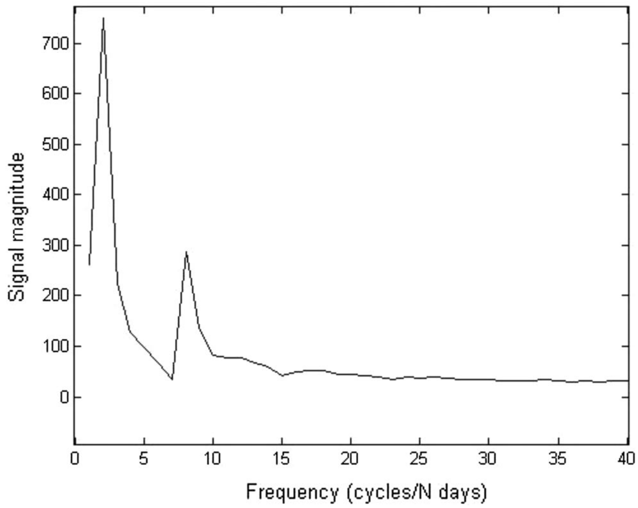

Fig. 2 **DSCOVR fuel-tank temperature frequency magnitudes.**

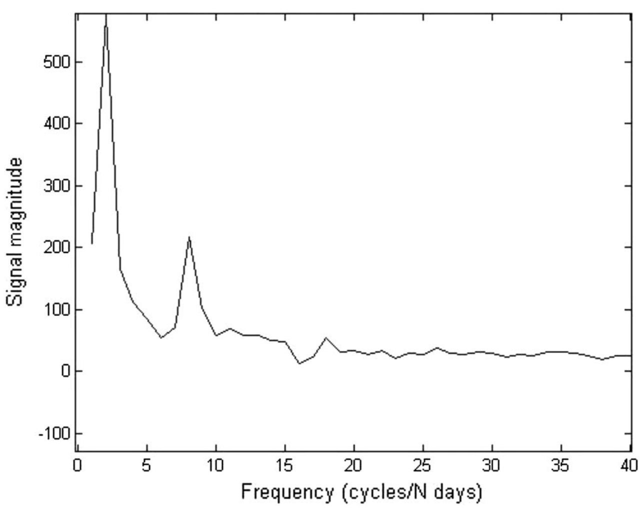

Fig. 3 **DSCOVR comphub-temperature frequency magnitudes.**

ecliptic distance has eight extrema during the time period used in this study, which corresponds to the 83.75-day cycle.

Because DSCOVR points toward Earth throughout its orbit, its attitude with respect to the sun will change at different points in the orbit, and will thus expose different portions of the spacecraft to sunlight. Changes in pitch are accounted for by DSCOVR's out-of-ecliptic distance. Roll and yaw are inversely related to each other, and have extrema with frequencies and phases near those of the temperature values. Figure 6 shows the yaw angle with respect to the temperatures. It can be seen that there are almost 16 extrema in the yaw data, which is near the 37.22-day cycle.

The sun–Earth–vehicle (SEV) angle has a strong correlation with the yaw, as seen in Fig. 7, but there are fewer jumps in values. Therefore, the SEV angle is used instead of yaw.

The fuel-tank temperature data were fit to several models. Table 1 shows the parameters included in each model, the correlation coefficients of the models, and the average errors between the modeled and observed values. From that information, the model that best fits the fuel-tank temperatures, Model T5, contains a constant term, distance between DSCOVR and the sun in the ecliptic plane, DSCOVR's out-of-ecliptic distance, a secular term, a secular-squared term, and the SEV angle. Figure 8 shows the temperatures based on this model and those based on observations. The model generally matches the temperature maximums, minimums, and phases, but there are discrepancies.

Table 2 shows the parameters for models based on comphub temperatures, along with the correlation coefficients and average errors. The model with the best performance, Model C5, contains a constant term, distance from the sun in the ecliptic plane, the squared out-of-ecliptic distance, a secular term, a secular-squared term, and the SEV angle. Figure 9 shows the modeled and observed comphub temperatures.

Because it was hoped that the models could be used to predict future temperature values, and because the model's prediction capability would indicate whether the chosen parameters were factors in the temperature values, some of the models were used to predict values from 1 May 2017 to 31 August 2017. The comparisons between the predicted and actual temperature values are shown in Table 3. The predicted comphub temperatures were closer to the actual temperatures than the predicted fuel-tank temperatures. In both cases, the model with the secular-squared term resulted in lower errors than the other models.

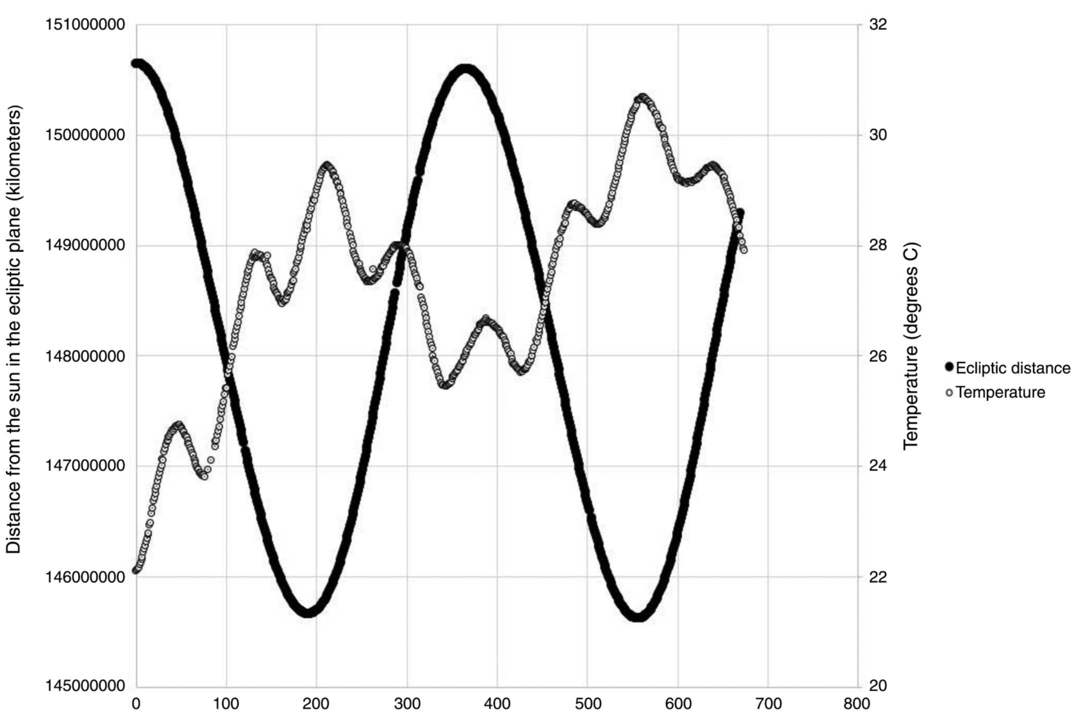

Fig. 4 **DSCOVR fuel-tank temperature and distance from the sun in the ecliptic plane.**

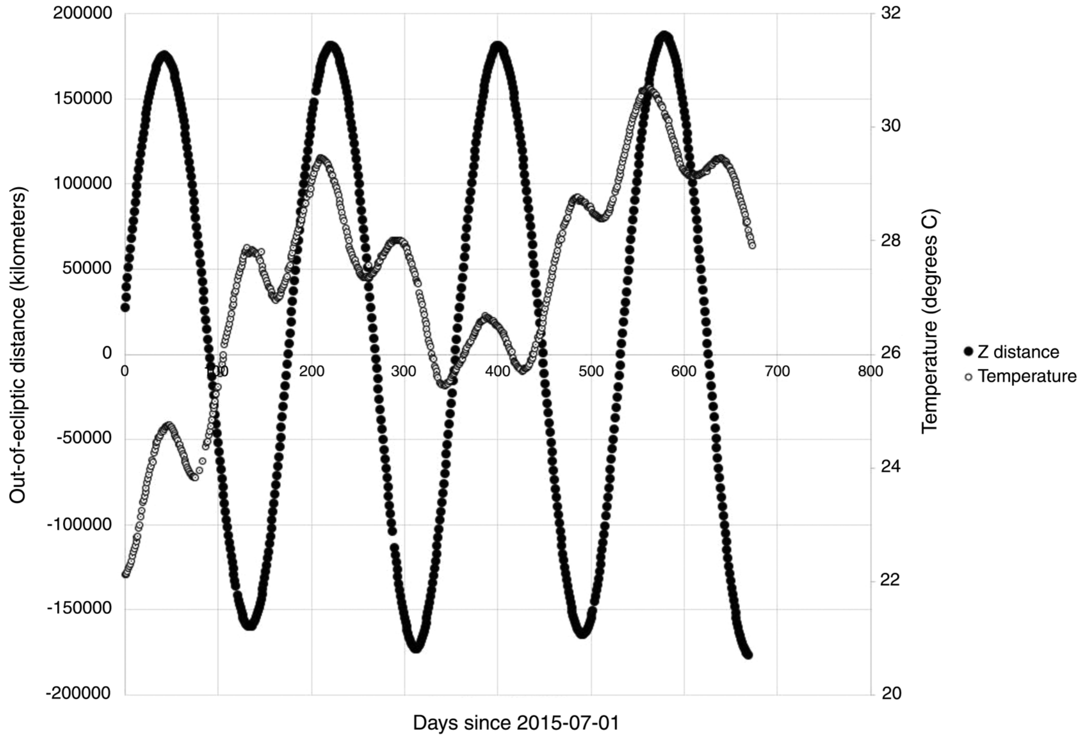

Fig. 5 DSCOVR fuel-tank temperature and out-of-ecliptic distance.

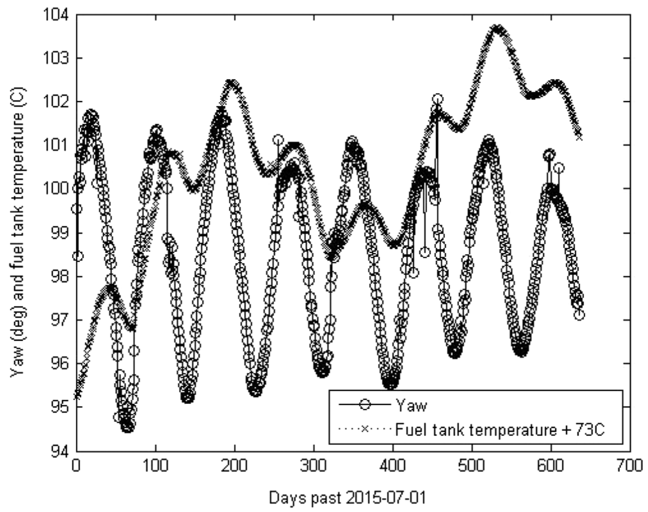

Fig. 6 DSCOVR fuel-tank temperature and yaw with respect to the sun.

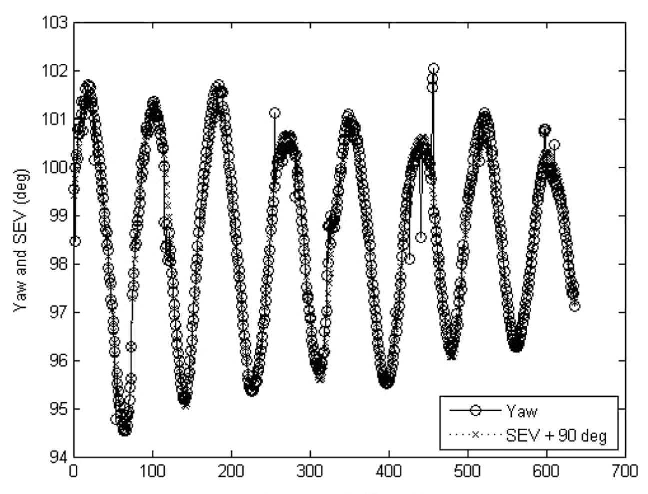

Fig. 7 DSCOVR SEV angle and yaw with respect to the sun.

Table 1 DSCOVR fuel-tank-temperature-model performances

Model	Correlation coefficient	Average error, °C
Model T1: constant and distance from the sun	0.56283	1.01280
Model T2: constant, distance from the sun in ecliptic, and out-of-ecliptic-distance squared	0.59349	0.98375
Model T3: constant, distance from the sun in ecliptic, out-of-ecliptic-distance squared, and secular	0.89006	0.50286
Model T4: constant, distance from the sun in ecliptic, out-of-ecliptic-distance squared, secular, and SEV angle	0.92811	0.41489
Model T5: constant, distance from the sun in ecliptic, out-of-ecliptic-distance squared, secular, secular squared, and SEV angle	0.94627	0.36680

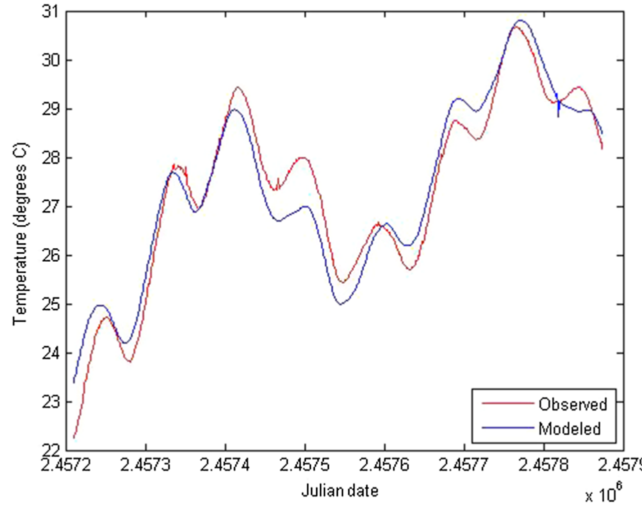

Fig. 8 DSCOVR modeled and observed tank temperatures; the model includes secular and constant terms, distance from the sun in the ecliptic, distance from the ecliptic, and SEV angle. DSCOVR modeled and observed tank temperatures for Model T5.

Table 2 DSCOVR comphub-temperature-model performances

Model	Correlation coefficient	Average error, °C
Model C1: constant and distance from the sun	0.61580	0.82129
Model C2: constant, distance from the sun in ecliptic, and out-of-ecliptic-distance squared	0.61613	0.72857
Model C3: constant, distance from the sun in ecliptic, out-of-ecliptic-distance squared, and secular	0.83507	0.48209
Model C4: constant, distance from the sun in ecliptic, out-of-ecliptic-distance squared, secular, and SEV angle	0.93252	0.25009
Model C5: constant, distance from the sun in ecliptic, out-of-ecliptic-distance squared, secular, secular squared, and SEV angle	0.95435	0.17196

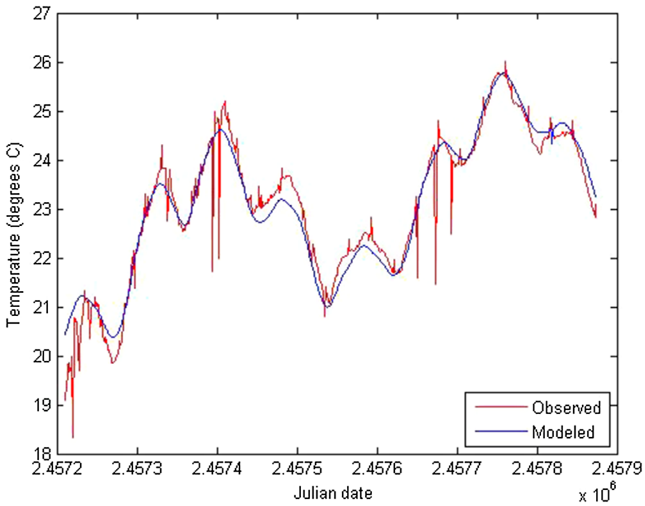

Fig. 9 DSCOVR modeled and observed comphub temperatures; the model includes secular and constant terms, distance from the sun in the ecliptic plane, distance from the ecliptic, and SEV angle with respect to the sun. DSCOVR modeled and observed comphub temperatures for Model C5.

Table 3 Fuel-tank- and comphub-temperature-model prediction errors

Model	Fuel-tank average absolute error, °C	Computation-hub average absolute error, °C
Constant, distance from the sun in ecliptic, out-of-ecliptic-distance squared, secular, and SEV angle	0.92476	0.52798
Constant, distance from the sun in ecliptic, out-of-ecliptic-distance squared, secular, secular squared, and SEV angle	0.39658	0.24974

Because the models with the secular-squared term made significantly better predictions than the other models, it implies that nonorbital factors have a significant effect on the fuel-tank and comphub temperatures. Potential factors could be degradation of MLI or of the spacecraft surfaces.

III. Conclusions

Changes in DSCOVR's fuel-tank and comphub temperatures appear to be caused mostly by its distance from the sun and its angle with respect to the sun. It is likely that degradation of the spacecraft's insulation and surfaces also contributes to increases in temperature throughout the life of the mission.

Models were created to predict the temperatures. The models with the lowest prediction errors contained terms for distance from the sun within the ecliptic, the square of the out-of-ecliptic distance, the sun–Earth–vehicle angle, secular and secular-squared terms, and a constant term. Those models had prediction errors of 0.39658°C for the fuel-tank temperature and 0.24974°C for the comphub temperature. Whereas the fuel-tank temperature prediction error is too high to improve predictions for maneuver performance, the comphub-temperature model will slightly improve the ability to predict when clock updates are needed.

Acknowledgments

The authors were contractors for the National Oceanic and Atmospheric Administration and the NASA. The authors would like to thank the reviewers and editors.

References

[1] Howell, K. C., and Pernicka, H. J., "Numerical Determination of Lissajous Trajectories in the Restricted Three-Body Problem," *Celestial Mechanics*, Vol. 41, Nos. 1–4, 1987, pp. 107–124. doi:10.1007/BF01238756

[2] Roberts, C., Case, S., Reagoso, J., and Webster, C., "Early Mission Maneuver Operations for the Deep Space Climate Observatory Sun-Earth L1 Libration Point Mission," *AIAA/AAS Astrodynamics Specialist Conference*, AIAA Paper 2015-0595, 2015, pp. 1–21.

[3] Garrick, J., "Attitude Control System Analysis Reports for Science Control Mode," NASA GSFC DSCOVR-ANYS-002170, Dec. 2014.

[4] Hawk, J., "Thermal Control System Users Guide," NASA GSFC DSCOVR-HDBK-002259, June 2015.

[5] Dever, J., Banks, B., de Groh, K., and Miller, S., "Degradation of Spacecraft Materials," *Handbook of Environmental Degradation of Materials*, edited by M. Kutz, William Andrew Publ., Norwich, NY, 2005, pp. 465–501, Chap. 23.

[6] Yoder, D., "Operations Concept Document," NASA GSFC DSCOVR-MGMT-000089, April 2014.

[7] Anon., "C&DH Clock Drift," NASA GSFC DSCOVR-PRES-002246, April 2014.

T. K. Minton
Associate Editor